

CYCLIC NONLINEAR BEHAVIOUR OF RC FRAMED STRUCTURES ACCOUNTING FOR FLEXURE-SHEAR INTERACTION

P. Ceresa¹, L. Petrini² and R. Pinho³

¹ Post-Doctoral Researcher, Dept. of Structural Mechanics, University of Pavia, Pavia, Italy

² Assistant Professor, Dept. of Structural Engineering, Politecnico of Milano, Milano, Italy

³ Assistant Professor, Dept. of Structural Mechanics, University of Pavia, Pavia, Italy

Email: ceresa@unipv.it, lorenza.petrini@polimi.it, rui.pinho@unipv.it

ABSTRACT :

Fibre beam-column elements thus far proved to be very accurate in the simulation of flexure dominated behaviour of reinforced concrete (RC) frames. However, when the shear span of the frame elements is small, the shear behaviour plays an important role in the overall response of the structure, as observed in numerous post-earthquake site observations. It is responsible for some of the most sudden and impressive failures of RC structures throughout earthquake-damaged areas. Whilst there are various modelling strategies in literature able to predict the shear response and the shear-flexure coupling under monotonic loading conditions, very few are the reported models that have demonstrated successful results under cyclic loading, as in the seismic load case. Accordingly, the present work aims at formulating and implementing, in a finite element code, a fibre beam-column model for predicting nonlinear behaviour in shear of RC framed structures. Numerical results obtained with this model are compared to experimental results. In particular, the cyclic behaviour of squat RC columns and shear walls are taken into account. It is found that the developed model is able to catch the main characteristics of the structural element shear response.

KEYWORDS: fibre element, shear deformations, seismic analysis, reinforced concrete frames

1. INTRODUCTION

Currently, the accurate simulation of behaviour of existing RC structures subjected to strong ground motion, and in particular the determination of shear strength and deformation response, is still a challenging and open problem. Most of the state-of-the-art on seismic design and assessment procedures proposed recently for common engineering practice requires either static or dynamic nonlinear analyses using frame elements where the nonlinearity is traditionally introduced with lumped-plasticity models, or distributed-inelasticity models (i.e., the so-called fibre beam-column elements). With the fibre modelling approach, the coupled axial and flexure effects are easily accounted for, while the flexural-shear coupling is not straightforward. Accordingly, only few modelling strategies (Ceresa *et al.*, 2007) have accounted for and implemented it up to now.

The work presented in this paper thus aims at formulating and implementing, in a finite element code, a fibre beam-column model for predicting nonlinear behaviour in shear of RC framed structures.. In order to reach this objective the work was organised in the following different phases, accurately described in the next sections: (i) choice of a reliable constitutive model for cracked RC subjected to cyclic loading, (ii) verification of the constitutive model using experimental data, (iii) development of a flexure-shear model for cracked RC beam-column elements, (iv) implementation of the formulation into a fibre beam-column element, and (v) verification of the model in predicting the experimental cyclic response of RC members.

2. THE ADOPTED CONSTITUTIVE FORMULATION

Several theories for cracked reinforced concrete subjected to shear are present in the literature. After a careful review of such literature, the Modified Compression Field Theory (MCFT) stood out as one of those models

that seemed capable of accurately predicting the shear strength of RC members subjected to monotonic loads (Vecchio and Collins, 1986; Vecchio, 2000). Indeed, the procedure (adopting membrane elements) has been shown to lead to quite accurate foresights when compared to experimental test results on RC panels and shear walls. The main assumption of MCFT is that cracked RC is treated as an orthotropic material where cracks are smeared and allowed to rotate; the principal strain-stress directions (1, 2) are those corresponding to the average compressive and tensile strains (crack directions). Analysis capability for cyclic loading conditions has been added by Vecchio (1999). The constitutive relations for concrete and reinforcing bars were expanded to account for cyclic loading and the plastic strains were introduced as offsets. The elastic components of strains were used to define the effective secant stiffnesses, and Mohr's circle technique was used to track strains experienced during previous loading. The MCFT formulation was adopted as the fibre constitutive model in the proposed modelling strategy, and its implementation was checked through a comparison with the experimental results and the predictions published by Vecchio *et al.* for several shear tests performed on RC panels at the University of Toronto. In the majority of the analysed cases, the MCFT theory proved to be capable of reproducing the fundamental aspects of the experimental responses for both monotonic and cyclic loading conditions. The accurate description of the implemented compatibility and equilibrium conditions, and of the hysteretic stress-strain relationships for concrete and for reinforcing bars, can be found in Ceresa (2007).

3. IMPLEMENTATION OF THE FLEXURE-SHEAR MODEL

Chosen the constitutive model, a two-dimensional Timoshenko fibre beam-column element was developed.

3.1 Section state determination

Considering a cross section discretised with n fibres, the stresses and strains of each i -th fibre are related by means of the following constitutive relations:

$$\begin{Bmatrix} \sigma_{xx} \\ \sigma_{yy} \\ \tau_{xy} \end{Bmatrix}^i = \begin{bmatrix} D_{11} & D_{12} & D_{13} \\ D_{21} & D_{22} & D_{23} \\ D_{31} & D_{32} & D_{33} \end{bmatrix}^i \begin{Bmatrix} \varepsilon_{xx} \\ \varepsilon_{yy} \\ \gamma_{xy} \end{Bmatrix}^i - \begin{Bmatrix} \sigma_{oxx} \\ \sigma_{oyy} \\ \tau_{oxy} \end{Bmatrix}^i \quad (3.1)$$

where $[D]^i$ is the total material stiffness matrix in the reference system x-y, and $\{\sigma\}_o^i$ is the pseudo-stress vector accounting for prestrains (i.e. plastic deformations, elastic offsets, strains due to shear slip). For the determination of the fibre strains, the hypotheses of plane section and uniform shear deformation along the section, according to the Timoshenko beam theory, are introduced. Hence, knowing the element deformations – axial deformation (ε_o), section curvature (χ) and shear deformation (γ_o) – it is possible to derive axial strain (ε_{xx}) and shear distortion (γ_{xy}) within each fibre. The only unknown is the transversal strain (ε_{yy}). Assuming that transversal stress within each fibre is equal to zero, ε_{yy} is iteratively determined as follows:

$$\sigma_{yy}^i = 0 \Rightarrow \varepsilon_{yy}^i = \left(-(\varepsilon_{xx} D_{21} + \gamma_{xy} D_{23}) / D_{22} + \sigma_{oyy} / D_{22} \right)^i \quad (3.2a)$$

$$\begin{Bmatrix} \sigma_{xx} \\ \tau_{xy} \end{Bmatrix}^i = \begin{bmatrix} k_{11} & k_{12} \\ k_{21} & k_{22} \end{bmatrix}^i \begin{Bmatrix} \varepsilon_{xx} \\ \gamma_{xy} \end{Bmatrix}^i + \begin{Bmatrix} -\sigma_{oxx} + \sigma_{oyy} \alpha_{12} \\ -\tau_{oxy} + \sigma_{oyy} \alpha_{32} \end{Bmatrix}^i \quad (3.2b)$$

where D_{21} , D_{22} , D_{23} are the coefficients of the total material matrix $[D]^i$, and σ_{oyy} is the transversal component of the pseudo-stress vector of Equation (3.1); k_{11} , k_{12} , k_{21} , k_{22} are the coefficients of the condensed composite material matrix (2×2), and $\alpha_{12} = D_{12}/D_{22}$, and $\alpha_{32} = D_{32}/D_{22}$.

It results that the transversal strain is expressed as a function of both axial and shear deformations and, additionally, of the transversal component σ_{yy} of the pseudo-stress vector where the plastic deformations are accounted for. Once the equilibrium in the transverse direction is achieved within a specific tolerance error for each fibre, the static condensation of Equation (3.1) leads to the determination of the axial and shear stresses for each fibre (Equation 3.2b). The condensed composite stiffness matrix establishes a direct coupling between the axial and the shear strains, and therefore between axial and shear stresses at sectional level.

3.2 Implementation of a Timoshenko fibre beam element

The developed two-dimensional fibre beam-column element was implemented in FEAPpv (Taylor, 2005). A classical displacement-based approach was followed. The three degrees of freedom (DOFs) per node – axial $u(x)$ and transversal $v(x)$ displacements, rotation $\theta_z(x)$ – were approximated through linear shape functions:

$$u(x) = \mathbf{N}^u(x) \cdot \hat{\mathbf{u}}, \quad v(x) = \mathbf{N}^v(x) \cdot \hat{\mathbf{v}}, \quad \theta_z(x) = \mathbf{N}^{\theta_z}(x) \cdot \hat{\theta}_z \quad (3.3)$$

where $\hat{\mathbf{u}}$, $\hat{\mathbf{v}}$ and $\hat{\theta}_z$ are the nodal DOFs and x is the beam axis. The beam cross-section is in the y - z plane and length is l . In order to overcome the shear-locking phenomenon (Prathap and Bhashyam, 1982), the shape function for the transversal displacement was enriched with the addition of a linked term, or *bubble function* $N_b = 0.5 \cdot (1 - x/l) \cdot (x/l)$, and the derived shear deformation is computed as follows (Auricchio, 2003):

$$\begin{aligned} v(x) &= \mathbf{N}^v(x) \hat{\mathbf{v}} + N_b (\hat{\theta}_{z1} - \hat{\theta}_{z2}) l = \mathbf{N}^v(x) \hat{\mathbf{v}} + N_b l (\mathbf{b} \cdot \hat{\theta}_z) \\ \rightarrow \gamma_{xy}(x) &= \mathbf{B}^v(x) \hat{\mathbf{v}} - \mathbf{N}^{\theta_z}(x) \hat{\theta}_z + \mathbf{D}_b(x) \hat{\theta}_z \end{aligned} \quad (3.4)$$

with the introduction of the following quantities: $\mathbf{b} = (1, -1)$, $\hat{\theta}_z = (\hat{\theta}_{z1}, \hat{\theta}_{z2})^T$, $\mathbf{D}^b(x) = 0.5 \cdot (1 - 2x/l) \mathbf{b}$.

The element stiffness matrix is computed by means of linearisation of the residual functions with respect to the nodal displacements; hence the following terms (2×2 sub-matrices) are derived:

$$\begin{aligned} \mathbf{K}_{uu} &= \int_l \int_A (\mathbf{B}^u)^T \frac{\partial \sigma_{xx}}{\partial \varepsilon_{xx}} \mathbf{B}^u dA dl; & \mathbf{K}_{uv} &= \int_l \int_A (\mathbf{B}^u)^T \frac{\partial \sigma_{xx}}{\partial \gamma_{xy}} \mathbf{B}^v dA dl \\ \mathbf{K}_{u\theta} &= \int_l \int_A (\mathbf{B}^u)^T \frac{\partial \sigma_{xx}}{\partial \varepsilon_{xx}} y (-\mathbf{B}^{\theta_z}) dA dl + \int_l \int_A (\mathbf{B}^u)^T \frac{\partial \sigma_{xx}}{\partial \gamma_{xy}} [-\mathbf{N}^{\theta_z} + \mathbf{D}^b] dA dl \\ \mathbf{K}_{vu} &= \int_l \int_A (\mathbf{B}^v)^T \frac{\partial \tau_{xy}}{\partial \varepsilon_{xx}} \mathbf{B}^u dA dl; & \mathbf{K}_{vv} &= \int_l \int_A (\mathbf{B}^v)^T \frac{\partial \tau_{xy}}{\partial \gamma_{xy}} \mathbf{B}^v dA dl \\ \mathbf{K}_{v\theta} &= \int_l \int_A (\mathbf{B}^v)^T \frac{\partial \tau_{xy}}{\partial \varepsilon_{xx}} (-y \mathbf{B}^{\theta_z}) dA dl + \int_l \int_A (\mathbf{B}^v)^T \frac{\partial \tau_{xy}}{\partial \gamma_{xy}} [-\mathbf{N}^{\theta_z} + \mathbf{D}^b] dA dl \\ \mathbf{K}_{\theta u} &= \int_l \int_A (\mathbf{B}^{\theta_z})^T \frac{\partial \sigma_{xx}}{\partial \varepsilon_{xx}} (-y \mathbf{B}^u) dA dl + \int_l \int_A [\mathbf{D}^b - \mathbf{N}^{\theta_z}]^T \frac{\partial \tau_{xy}}{\partial \varepsilon_{xx}} (\mathbf{B}^u) dA dl \\ \mathbf{K}_{\theta v} &= \int_l \int_A (\mathbf{B}^{\theta_z})^T \frac{\partial \sigma_{xx}}{\partial \gamma_{xy}} (-y \mathbf{B}^v) dA dl + \int_l \int_A [\mathbf{D}^b - \mathbf{N}^{\theta_z}]^T \frac{\partial \tau_{xy}}{\partial \gamma_{xy}} (\mathbf{B}^v) dA dl \\ \mathbf{K}_{\theta\theta} &= \int_l \int_A (\mathbf{B}^{\theta_z})^T \left\{ \frac{\partial \sigma_{xx}}{\partial \varepsilon_{xx}} (y^2 \mathbf{B}^{\theta_z}) + \frac{\partial \sigma_{xx}}{\partial \gamma_{xy}} (-y) [\mathbf{D}^b - \mathbf{N}^{\theta_z}] \right\} dA dl + \end{aligned}$$

$$\int_l \int_A [\mathbf{D}^b - \mathbf{N}^{\theta z}]^T \left\{ \frac{\partial \tau_{xy}}{\partial \varepsilon_{xx}} (-y \mathbf{B}^{\theta z}) + \frac{\partial \tau_{xy}}{\partial \gamma_{xy}} [\mathbf{D}^b - \mathbf{N}^{\theta z}] \right\} dA dl$$

where the coefficients $\partial \sigma_{xx} / \partial \varepsilon_{xx}$, $\partial \sigma_{xx} / \partial \gamma_{xy}$, $\partial \tau_{xy} / \partial \gamma_{xy}$, and $\partial \tau_{xy} / \partial \varepsilon_{xx}$ are derived from the static condensation in Equation (3.2a). These terms are different from zero due to the adopted flexure-shear fibre model. Therefore, the stiffness matrix directly includes the coupling between flexure and shear contributions. Moreover, the presence of the bubble function introduces additional terms in the stiffness matrix coefficients.

4. NUMERICAL VERIFICATION OF THE FLEXURE-SHEAR MODEL

The proposed modelling strategy was verified by means of comparisons with experimental responses of RC columns and shear walls subjected to cyclic loading. The results of the developed fibre-shear formulation are also compared with the ones obtained with a fibre-flexural formulation (SeismoStruct, 2005).

4.1 Verification against experimental results on short piers with non-hollow cross section

The flexure-shear formulation was firstly validated by modelling RC squat columns with full cross-section (labelled as "Col_Solid_"). The numerical predictions of three case-studies are presented in the following. The first application refers to the RC column (Column OA5) tested in Japan by Arakawa *et al.* (1989); a further simulation makes use of the tests conducted in Japan by Imai and Yamamoto (1986); the third case (Column SC3) is related to the tests performed at the University of Texas by Aboutaha *et al.* (1999). In the following, the specimens will be named after their aspect ratio as: Col_Solid_1.25, Col_Solid_1.65, Col_Solid_2.67, respectively. The applied axial loads, the geometric and mechanical properties of the case studies are given in Table 4.1. The force-displacement responses are plotted from Figure 1 to Figure 3.

Table 4.1 Geometrical and material parameters for solid and hollow cross-section squat RC columns

	Col_Solid_1.25 L = 225mm	Col_Solid_1.65 L = 825mm	Col_Solid_2.67 L = 1219.2mm	Col_Hollow_1.75 L = 2800 mm	Col_Hollow_1.75 L = 2800 mm
Reference	Arakawa <i>et al.</i> ⁽¹⁹⁸⁹⁾	Imai and Yamamoto ⁽¹⁹⁸⁶⁾	Aboutaha <i>et al.</i> ⁽¹⁹⁹⁹⁾	Pinto <i>et al.</i> ⁽¹⁹⁹⁵⁾	Calvi <i>et al.</i> ⁽²⁰⁰⁵⁾
Scale factor	1:2	1:2	1:1	1:1	1:4
$b \times h$ (mm)	180 × 180	400 × 500	914.4 × 457.2	800 × 1600 480 × 1280	450 × 450 300 × 300
N (kN)	-476	-392	-	-1700	-250
f'_c (MPa)	-33.0	-27.1	-21.9	-35.4	-35.0
E_c (MPa)	26999	24467	21995	27964	27806
f'_t (MPa)	1.89	1.72	1.54	1.96	1.95
Long. Bars	8 ϕ 12.7	14 ϕ 22	4 ϕ 25.5 + 12 ϕ 25	40 ϕ 8 + 28 ϕ 12 + 12 ϕ 10	24 ϕ 8
f_{y_long} (MPa)	340	318	434	503 & 558 & 489	520
Stirrups	ϕ 4 @ 64.3	ϕ 9 @ 100	ϕ 9.53 @ 406.4	ϕ 5 @ 60	ϕ 3 @ 75
f_{y_stir} (MPa)	249	336	400	700	710

Comparisons with the experimental results show significant improvement in response predictions when the flexural formulation is replaced by the developed fibre-shear formulation. Even if the latter leads to an overestimation of the initial stiffness and an exaggerating pinching effect, the predicted response shows a better agreement with the measured behaviour in terms of both energy dissipation and shear capacity. The experimentally observed lateral strength degradation is well captured for specimens Col_Solid_1.25 and Col_Solid_1.65, whereas the ultimate lateral load is not well reproduced for the Col_Solid_2.67 case-study.

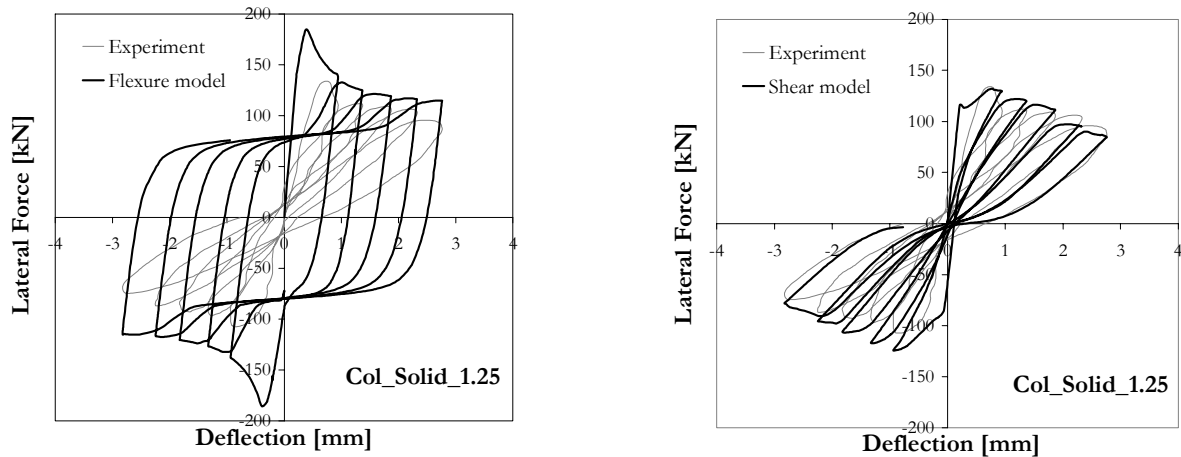


Figure 1 Force-displacement response of specimen Col_Solid_1.25 (Arakawa *et al.*, 1989) using fibre-flexure model (on the left), and the implemented fibre-shear model (on the right)

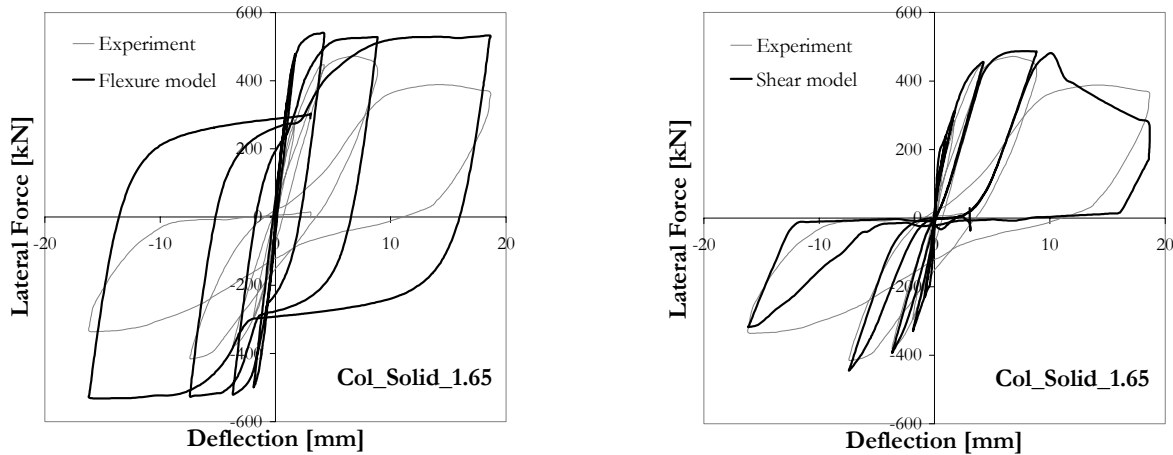


Figure 2 Force-displacement response of specimen Col_Solid_1.65 (Imai and Yamamoto, 1986) using fibre-flexure model (on the left), and the implemented fibre-shear model (on the right).

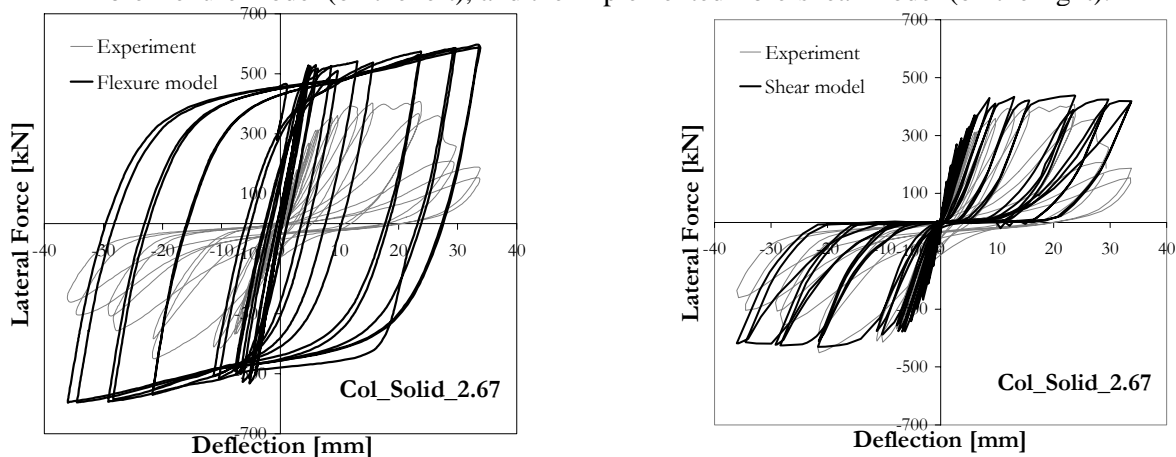


Figure 3 Force-displacement response of specimen Col_Solid_2.67 (Aboutaha *et al.*, 1999) using fibre-flexure model (on the left), and the implemented fibre-shear model (on the right)

4.2 Verification against experimental results on short piers with hollow cross section

A second set of analyses focused on modelling the response of squat RC columns with hollow cross-section (labelled as “Col_Hollow_”). Two case-studies are presented: the pier tested by Pinto *et al.* (1995) at the

European Laboratory for Structural Assessment (ELSA) – Col_Hollow_1.75 – and one of the piers tested at the University of Pavia (Calvi *et al.*, 2005) – Col_Hollow_2.0. Geometry and material properties of these two columns are summarised in Table 4.1. The force-displacement responses are plotted in Figure 4 and Figure 5.

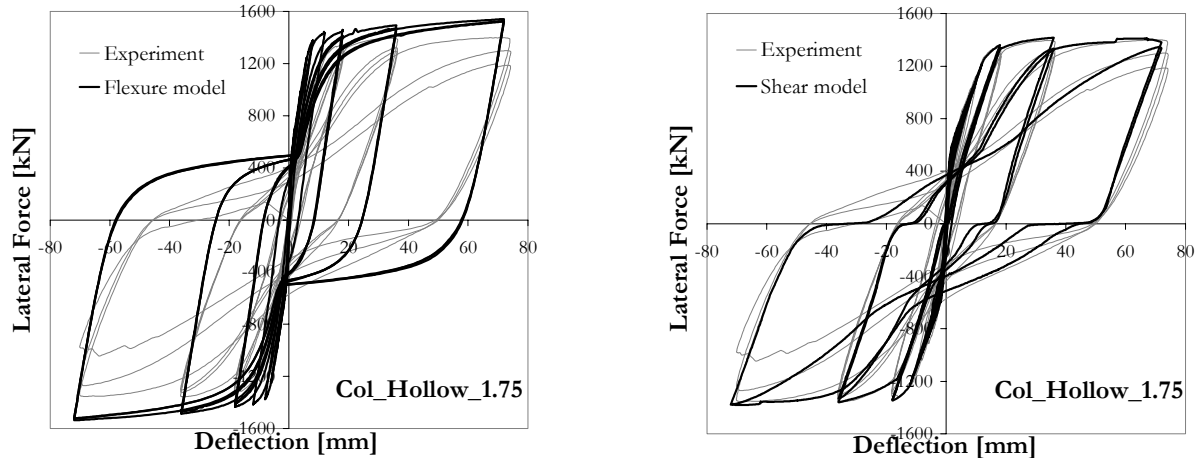


Figure 4 Force-displacement response of specimen Col_Hollow_1.75 (Pinto *et al.*, 1995) using fibre-flexure model (on the left), and the implemented fibre-shear model (on the right)

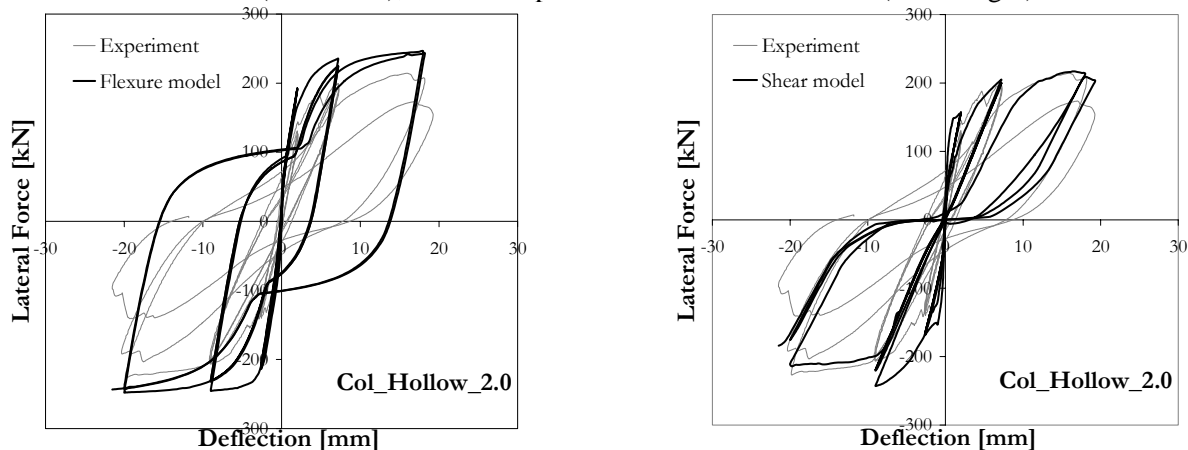


Figure 5 Force-displacement response of specimen Col_Hollow_ (Calvi *et al.*, 2005) using fibre-flexure model (on the left), and the implemented fibre-shear model (on the right)

The developed modelling strategy seems to be capable of reproducing the measured responses in a satisfactory way, mainly for the Col_Hollow_1.75. Despite the overestimation of the initial stiffness in specimen Col_Hollow_2.0, the flexure-shear model still leads to improved predictions of the overall response if compared with the predictions obtained with the flexural fibre model. However, the model is not able to capture well the degradation of the strength and stiffness for high ductility levels.

4.3 Verification against experimental results on walls

The performance of the developed modelling strategy was also assessed against the results of two RC structural walls (labelled as “Wall_”): the specimen (SW35) tested by Elnashai and Salama (1992) at the Imperial College London (Wall_2.0) and one of the RC walls (WSH3) tested by Dazio *et al.* (1999) at the Swiss Federal Institute of Technology of Zurich (Wall_2.28). The geometry and the mechanical properties of the two walls are given in Table 4.2. The numerical simulation results are shown in Figure 6 and Figure 7. Once again, it can be observed that the fibre-shear model allows the experimental results to be reproduced with relatively good accuracy, this time without a conspicuous initial stiffness overestimation, as had been observed for the case of columns.

Table 4.2 Geometry and material parameters for RC shear walls

	Wall_2.0 L = 1200 mm	Wall_2.28 L = 4560 mm
Reference	Elnashai and Salama ⁽¹⁹⁹²⁾	Dazio <i>et al.</i> ⁽¹⁹⁹⁹⁾
Scale factor	1:2.5	1:2
Outer perimeter $b_w \times l_w$ (mm)	60 × 600	150 × 2000
N (kN)	-0.2	-626
f'_c (MPa)	48.4	39.4
E_c (MPa)	32698	35700
f'_t (MPa)	2.29	2.07
Web - Long. bars	6 ϕ 12 + 4 ϕ 6	22 ϕ 8
f_{y_long} (MPa) of ϕ 8	450	700.2
Edge - Long. bars	4 ϕ 8 + 2 ϕ 12	6 ϕ 12
f_{y_long} (MPa) of ϕ 12	450	725.5
Web - Stirrups	ϕ 5 @ 60	ϕ 6 @ 150
Edge - Stirrups	ϕ 5 @ 60 + ϕ 5 @ 20	ϕ 6 @ 150 + ϕ 6 & ϕ 4.2 @ 75
f_{y_stir} (MPa) of ϕ 6	450	615

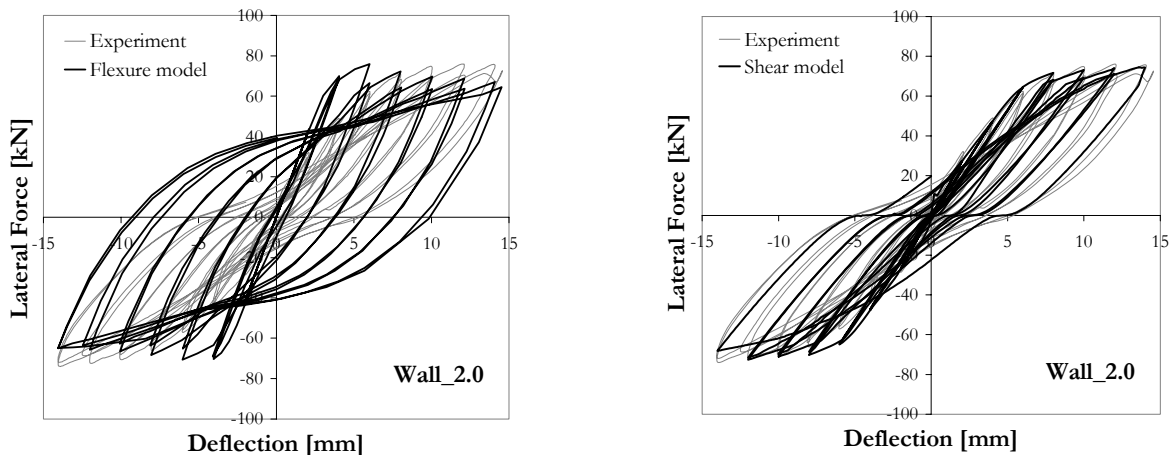


Figure 6 Force-displacement response of specimen Wall_2.0 (Elnashai and Salama, 1992) using fibre-flexure model (on the left), and the implemented fibre-shear model (on the right)

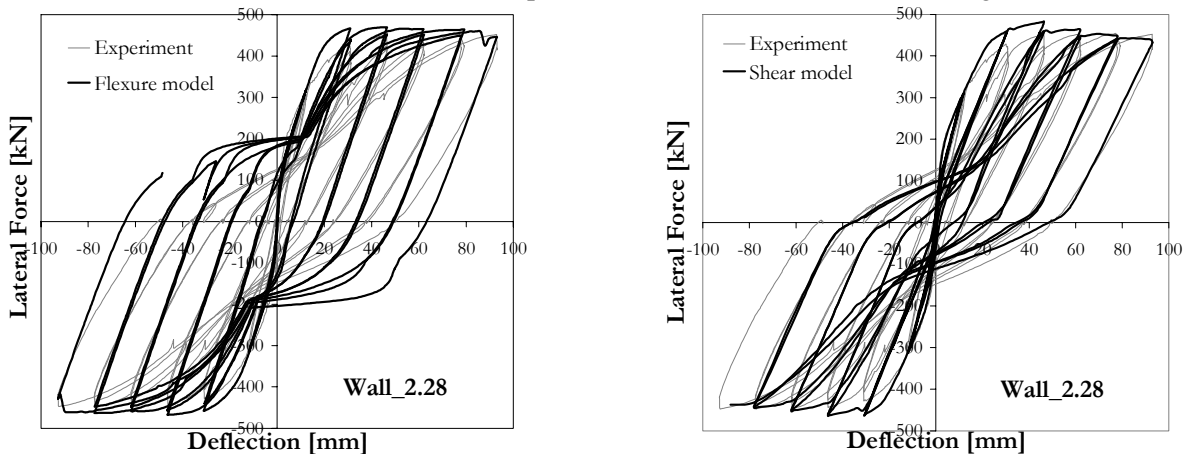


Figure 7 Force-displacement response of specimen Wall_2.28 (Dazio *et al.*, 1999) using fibre-flexure model (on the left), and the implemented fibre-shear model (on the right)

5. CONCLUSIONS

The present research featured the objective of developing a fibre flexure-shear model for seismic analysis of reinforced concrete framed structures. Comparisons with experimental results on shear-sensitive elements (short piers and walls) showed relatively good accuracy in response predictions when using the developed fibre-shear formulation. The latter did not require empirical test-matching calibration; only engineering parameters (e.g. material strengths, reinforcement geometrical ratios) are required as input.

Nevertheless, post-peak strength degradation is not yet fully captured; in some cases pinching phenomenon is overestimated. Hence, the constitutive model implemented for concrete requires additional improvements; e.g. better post-peak behaviour and a crack-closing model. Bar buckling, dowel effect and crack-bridging should be introduced into the formulation. Then, additional experimental testing is necessary to corroborate the cyclic relationships for concrete in tension and for developing a plastic tensile offset model. Finally, extension to 3D loading is also to be carried out. In other words, notwithstanding the relatively satisfactory results, it is recognized that further research work and developments are required.

ACKNOWLEDGEMENTS

The authors are grateful to Prof. F. Auricchio for his assistance in the model implementation and to R. Sousa for the performed analyses. The authors also thank J. Bairan, C. Christopoulos, A. Correia, P. Kotronis, L. Martinelli, P. Mergos, D. Palermo, P. Pegon, A. Pinto and M. Remino for the valuable assistance in retrieving experimental data, supplying bibliographic material, and so on.

REFERENCES

- Aboutaha, R.S., Engelhardt, M.D., Jirsa J.O. and Kreger, M.E. (1999). Rehabilitation of shear critical concrete columns by use of rectangular steel jackets. *ACI Structural Journal* **96:1**, 68-78.
- Arakawa, T., Arai, Y., Mizoguchi, M. and Yoshida, M. (1989). Shear resisting behaviour of short reinforced concrete columns under biaxial bending-shear. *Transactions of the Japan Concrete Institute* **11**, 317-324.
- Auricchio, F. (2003). Nonlinear finite element analysis. *Class Notes*, ROSE School, Pavia Italy.
- Calvi, G.M., Pavese, A., Rasulo, A., Bolognini, D. (2005). Experimental and numerical studies on the seismic response of R.C. hollow bridge piers. *Bulletin of Earthquake Engineering* **3**, 267-297.
- Ceresa, P., Petrini, L., Pinho, R. (2007). Flexure-shear fibre beam-column elements for modelling frame structures under seismic loading- State of the art. *Journal of Earthquake Engineering* **11:1**, 46-88.
- Ceresa, P. (2007). Development of a fibre flexure-shear model for seismic analysis of RC framed structures. *PhD Thesis*, University of Pavia, Pavia, Italy.
- Dazio, A., Wenk, T. and Bachmann, H. (1999). Versuche an Stahlbetontragwänden unter zyklisch-statischer Einwirkung. *IBK Bericht N° 239*, ETH Zurich. Basel: Birkhauser Verlag (in German).
- Elnashai, A.S. and Salama, A.I. (1992). Selective repair and retrofitting techniques for RC structures in seismic regions. *Research Report ESEE/92-2*, Imperial College, London.
- Imai, H. and Yamamoto, Y. (1986) A Study on Causes of Earthquake Damage of Izumi High School Due to Miyagi-Ken-Oki Earthquake in 1978. *Transactions of the Japan Concrete Institute* **8**, 405-418.
- Pinto, A.V., Verzeletti, G., Negro, P. and Guedes, J. (1995). Cycling Testing of a Squat Bridge Pier. *Report EUR 16247 EN*, EC, JRC, Ispra, Italy.
- Prathap, G. and Bhashyam, G.R. (1982). Reduced integration and the shear flexible beam element. *International Journal of Numerical Methods Engineering* **18**, 195-210.
- SeismoSoft (2005). SeismoStruct - A computer program for static and dynamic nonlinear analysis of framed structures. Available from URL: www.seismosoft.com
- Taylor, R.L. (2005). FEAPPV – A Finite Element Analysis Program: Personal Version. Available from URL: www.ce.berkeley.edu/~rlt/feappv/
- Vecchio, F.J. (1999). Towards Cyclic Load Modelling of Reinforced Concrete. *ACI Structural Journal* **96:2**, 193-202.
- Vecchio, F.J. (2000). Disturbed Stress Field Model for Reinforced Concrete: Formulation. *Journal of Structural Engineering* **126:9**, 1070-1077.